JOURNAL OF COMPUTATIONAL PHYSICS 74, 244–262 (1988)

Numerical Simulation for Certain Stochastic Ordinary Differential Equations*

RENATO SPIGLER†

Courant Institute of Mathematical Sciences, New York University, New York, New York 10012

Received July 17, 1985; revised February 26, 1987

A Monte Carlo simulation approach is presented for solving two problems based on stochastic ordinary differential equations, namely an *initial-value* problem for a nonlinear ordinary differential equation *and* a two-point *boundary-value* problem for a linear equation. The method consists of simulating on the computer several realizations of the random process which appears in the coefficients of the equations, and then computing the average over the corresponding solutions. Since these two problems are related to the same physical problem, we are able to compare the results. Several plots are given to illustrate the results and a discussion of the various kinds of errors which affect the method is presented.

1. INTRODUCTION

The purpose of this paper is to illustrate, by some examples, a Monte Carlo approach to numerically treat (a) an initial-value (IV) problem for a *nonlinear* stochastic ordinary differential equation (SODE), and (b) a two-point boundary-value (BV) problem for a *linear* SODE. The approach consists of simulating on the computer several realizations of the stochastic process which enters the coefficients of the equations, and then evaluating the average over the corresponding solutions. As the underlying physical problem is the same in the two cases, we shall be able to compare the results of (a) and (b). The procedures described here are more than examples, as they can be applied to more general IV-problems and BV-problems for SODEs.

We start, in Section 2, with a short description of the physical problem and derive the equations to be numerically treated. Section 3 is divided into two parts: In Section 3a we give the details about the treatment of problem (a), while the same is done for problem (b) in Section 3b. Several graphs are then shown to

* This work was supported, in part, by the Air Force Office for Scientific Research, under Grant AFOSR-80-0228, a NATO fellowship, and the U. S. Department of Energy, under Grant DE-FG02-86-ER53223.

† This work was mostly written when the author was a Fulbright Scholar, on leave from the University of Padova. Permanent address: Università di Padova, Istituto di Matematica Applicata, via Belzoni 7, 35131 Padova, Italy.

0021-9991/88 $3.00

illustrate the results. Finally, in Section 4 we discuss the various types of numerical errors that affect our computations and in Section 5 we summarize the major points of the paper.

In [13] we studied essentially the same physical problem by using a completely different technique. We numerically solved a parabolic partial differential equation which describes the same statistical phenomenon considered here, but in a specific limit.

2. The Original Problem

When a plane electromagnetic wave propagates in a stratified lossless dielectric medium located in $0 < x < l$, along the direction of stratification, its electric field $u(x)$ satisfies an equation such as

$$u_{xx} + k_0^2 f(x)\, u = 0, \qquad 0 < x < l, \tag{2.1}$$

where $k_0 = \omega_0/c$ is the free-space wave number, ω_0 is the frequency, c is the speed of light in vacuum, and the dependence on time $\sim e^{-i\omega_0 t}$ has been omitted.

In the case where the medium is "random," i.e., only a statistical description of its properties is given, the dielectric function, $f(x)$, becomes a stochastic process, say, for example,

$$f(x, \omega) = 1 + \varepsilon\mu(x, \omega), \tag{2.2}$$

where $\varepsilon > 0$ is a small parameter and $\mu(x, \omega)$ is a suitable stochastic process on some probability space $(\Omega, \mathscr{A}, P)$; $\omega \in \Omega$ denotes the "chance."

While the numerical algorithm below can be implemented for *arbitrary* statistical properties of μ, here we make *certain specific* assumptions. On the one hand, these allow us to carry out all the computations, in practice; on the other hand they correspond to some suitable physical picture. More precisely, we assume $\mu(x, \omega)$ to be a zero-mean, wide-sense stationary, almost-surely bounded real-valued random function. The process $\mu(x, \omega)$ is also assumed to satisfy a "mixing condition," in a sufficiently strong sense (see, e.g., [5]). The dielectric function in (2.1) models, therefore, a large class of random media: media with $\mu(\cdot, \cdot)$ a finite state ergodic Markov chain, for example, are included (cf. [5]).

We shall take as a realization of $\mu(x, \omega)$ a piecewise constant function of x, equal to ± 1 in each section of length Δ, in which we divide the x-interval, the sign being chosen at random: This is the so-called "random telegraph" process, a two-state Markov process. Moreover, we shall choose the two-point correlation function for μ, say $\rho(z)$,

$$\rho(z) = \begin{cases} 1 - |z|/\Delta, & |z| \leqslant \Delta, \\ 0, & |z| > \Delta, \end{cases} \tag{2.2'}$$

which corresponds to a *uniform distribution* of the values ± 1 above. The choice (2.2) means that we represent the dielectric function of the medium as a small random perturbation around a mean value, taken equal to one.

Under these conditions, u becomes a stochastic process as well. In what follows the dependence on the chance ω will be omitted, as is customary.

Equation (2.1) also describes the propagation of TEM (two-wire) waves along certain transmission lines and the propagation of the fundamental mode in waveguides with random inhomogeneities.

Equation (2.1) must be considered together with the *boundary conditions*

$$\begin{aligned} &u(0) = T(l), && u_x(0) = -ik_0 T(l), \\ &u(l) = 1 + R(l), && u_x(l) = -ik_0[1 - R(l)], \end{aligned} \tag{2.3}$$

which state the continuity of the field and its derivative across the borders of the slab at $x = 0$ and $x = l$. Here $T(l)$ and $R(l)$ represent the complex-valued transmission and reflection coefficients; the incoming and the outgoing waves are assumed to be plane waves of the form

$$\begin{aligned} &u_1(x) = e^{-ik_0(x-l)} + R(l)\, e^{ik_0(x-l)}, && x > l, \\ &u_2(x) = T(l)\, e^{-ik_0 x}, && x < 0. \end{aligned}$$

By eliminating $T(l)$, $R(l)$ from (2.3) we obtain two boundary conditions involving u, u_x only:

$$\begin{aligned} &u_x(0) + ik_0 u(0) = 0 \\ &u_x(l) - ik_0 u(l) = -2ik_0. \end{aligned} \tag{2.3'}$$

Obtaining $T(l)$, $R(l)$, or better the mean powers $\langle |T(l)|^2 \rangle$, $\langle |R(l)|^2 \rangle = 1 - \langle |T(l)|^2 \rangle$, amounts to describing some of the scattering properties of the slab $0 < x < l$ and can be considered the first goal in studying wave propagation in random media. Now, it has been shown that, in the problem described above, $R(l)$ satisfies a nonlinear ODE, the Riccati equation

$$\frac{dR(l)}{dl} = 2ik_0 R(l) + \frac{ik_0}{2} \varepsilon\mu(l)(R(l) + 1)^2, \tag{2.4}$$

associated with the *initial condition*

$$R(0) = 0 \tag{2.4'}$$

(cf. e.g., [1, 2, 10]).

Note that from (2.3) it follows that

$$R(l) = u(l) - 1. \tag{2.5}$$

Therefore, our goal to compute $R(l)$ can be achieved by solving the *linear* BV-problem (2.1), (2.3′) as well as the *nonlinear* IV-problem (2.4), (2.4′). These are problems (b) and (a), respectively, which we want to treat numerically. More precisely, we want to obtain $\langle |R|^2 \rangle$ and $\langle |T|^2 \rangle$ by performing numerical simulation experiments. Something similar for problem (b) was done in [6, 8, 9]. However, a detailed description was not given nor was a discussion of the errors included.

We remark that coping with IV-problems such as (2.4), (2.4′) is more favorable, for numerical purposes, even in the corresponding deterministic problems.

3. Numerical Treatment

In this section we describe the treatment of the aforementioned problems (a) and (b) and show the corresponding results in several graphs. We divide the presentation into two subsections, according to the two problems.

3a. *Numerical Simulation for a Nonlinear IV-Problem for a* SODE

We generate "at random" on the computer a set, say, of N realizations of the process $\mu(x) \equiv \mu(x, \omega)$, and solve (2.4), (2.4′) for each of them. Then we evaluate the average over such N solutions, for each x.

More precisely, we divide the interval $[0, l_{\max}]$, for a given chosen value $l_{\max} > 0$ (the maximum slab width for which we wish to compute $\langle |R(l)|^2 \rangle$), in p sections of equal length $\Delta = l_{\max}/p$ and take as a realization of $\mu(x, \omega)$ a piecewise constant function, as described in Section 2. For the nth realization, $1 \leqslant n \leqslant N$, we evaluate $R_n(l_j)$, $l_j = j\Delta$, $j = 1, 2, ..., p$. Then we compute the average

$$\frac{1}{N} \sum_{n=1}^{N} |R_n(l_j)|^2, \tag{3a.1}$$

for $j = 1, 2, ..., p$.

When the problem can be idealized in such a way that the random perturbations have size ε so small as to let $\varepsilon \to 0$, and the slab is so thick or the transmission line or guide is so long as to let $l \to \infty$, it is possible to perform a rigorous analysis based on some limit-theorem from Probability Theory, due to Kahsminskii [4], provided that $\varepsilon \to 0$, $l \to \infty$, with $\varepsilon^2 l = \text{const}$. This is the so-called diffusion limit. Information can be obtained for the limiting-solution, in this case. In such a limiting theory, there appears naturally the scaled independent variable

$$\tau \equiv s\varepsilon^2 l \equiv \frac{l}{\chi}, \qquad s \equiv \frac{k_0^2}{2} \int_0^\infty \rho(z) \cos 2k_0 z \, dz, \tag{3a.2}$$

where

$$\rho(|x - y|) = \langle \mu(x) \, \mu(y) \rangle$$

is the two-point *correlation function* of the process $\mu(x)$, and s represents, essentially, its *power spectral density*.

In order to make a meaningful comparison with this theory, we rewrite (2.4) with the variable τ. Setting for short,

$$\alpha \equiv 2k_0, \qquad \beta(\tau) \equiv \frac{k_0}{2}\,\varepsilon\mu(\chi\tau), \tag{3a.3}$$

we obtain

$$\frac{dR}{d\tau} = i\alpha\chi R + i\chi\beta(R+1)^2, \qquad 0 < \tau < \tau_{\max}, \tag{3a.4}$$

for $R \equiv R(\chi\tau)$, where $\tau_{\max} = l_{\max}/\chi$.

Now, on the interval $[0, \tau_{\max}]$ divided in p sections of equal length $\delta = \tau_{\max}/p = \Delta/\chi$, we approximate $\beta(\tau)$ with the constant value $\beta_j \equiv \beta(\tau_j)$, $\tau_j \equiv j\delta$ in $[j\delta, (j+1)\,\delta)$, for $j = 0, 1, 2, \ldots, p-1$. We can solve *explicitly* (3a.4) in each interval $[j\delta, (j+1)\,\delta)$. Separating the variables in (3a.4) we obtain

$$\int_{R_j}^{R} \frac{dR}{R^2 + 2(1+2\eta_j)\,R + 1} = i\chi\beta_j(\tau - \tau_j), \qquad j\delta \leqslant \tau < (j+1)\,\delta. \tag{3a.5}$$

where $\beta_j \equiv \beta(j\delta) = (k_0/2)\,\varepsilon\mu(j\chi\delta)$, $R_j \equiv R(j\chi\delta)$, and

$$\eta_j \equiv \frac{k_0}{2\beta_j} = \frac{1}{\varepsilon\mu(j\chi\delta)}. \tag{3a.6}$$

As

$$R^2 + 2(1+2\eta_j)\,R + 1 = (R - R_+^j)(R - R_-^j), \tag{3a.7}$$

where

$$R_\pm^j = -(1+2\eta_j) \pm 2[\eta_j(1+\eta_j)]^{1/2} \tag{3a.8}$$

are real (and negative), we obtain from (3a.5)

$$\log\left(\frac{R - R_+^j}{R - R_-^j}\right)\Bigg|_{R_j}^{R} = i\chi\beta_j(R_+^j - R_-^j)(\tau - \tau_j),$$

i.e.,

$$\frac{R - R_+^j}{R - R_-^j} = \frac{R_j - R_+^j}{R_j - R_-^j}\exp\{i\chi\beta_j(R_+^j - R_-^j)(\tau - \tau_j)\},$$

and therefore the *explicit formula*

$$R(\chi\tau) = \frac{R_+^j - R_-^j \left(\frac{R_j - R_+^j}{R_j - R_-^j}\right) \exp\{i\chi\beta_j(R_+^j - R_-^j)(\tau - \tau_j)\}}{1 - \left(\frac{R_j - R_+^j}{R_j - R_-^j}\right) \exp\{i\chi\beta_j(R_+^j - R_-^j)(\tau - \tau_j)\}}, \qquad \tau_j \leqslant \tau < \tau_{j+1}, \tag{3a.9}$$

where $R_j \equiv R(j\chi\delta)$, $j = 0, 1, 2, ..., p-1$; $R_0 \equiv R(0) = 0$.

Observing that $R_+^j - R_-^j = 4[\eta_j(1+\eta_j)]^{1/2}$ and recalling that for numerical purposes we content ourselves with evaluating R at the discrete points $(j+1)\chi\delta$, we can write

$$R((j+1)\chi\delta) = \frac{R_+^j - R_-^j \left(\frac{R_+^j - R(j\chi\delta)}{R_-^j - R(j\chi\delta)}\right) \exp\left\{2\frac{ik_0}{\eta_j}\chi\delta[\eta_j(1+\eta_j)]^{1/2}\right\}}{1 - \left(\frac{R_+^j - R(j\chi\delta)}{R_-^j - R(j\chi\delta)}\right) \exp\left\{2\frac{ik_0}{\eta_j}\chi\delta[\eta_j(1+\eta_j)]^{1/2}\right\}}. \tag{3a.10}$$

As $R_-^j = 1/R_+^j$, (3a.10) can be written

$$R((j+1)\chi\delta) = R_+^j \frac{1 - \left(\frac{1 - R(j\chi\delta)/R_+^j}{1 - R(j\chi\delta)\,R_+^j}\right) \exp\left\{\frac{2ik_0}{\eta_j}\chi\delta[\eta_j(1+\eta_j)]^{1/2}\right\}}{1 - (R_+^j)^2 \left(\frac{1 - R(j\chi\delta)/R_+^j}{1 - R(j\chi\delta)\,R_+^j}\right) \exp\left\{\frac{2ik_0}{\eta_j}\chi\delta[\eta_j(1+\eta_j)]^{1/2}\right\}}. \tag{3a.10'}$$

Remark 3a.1. Formula (3a.10) (or (3a.10')) holds for arbitrary, not necessarily small, ε (as in the stochastic limit theory).

Remark 3a.2. For $j = 0$ we obtain from (3a.10), recalling that $R(0) = 0$,

$$R(\chi\delta) = \frac{R_+^0 \left[1 - \exp\left\{\frac{2ik_0}{\eta_0}\chi\delta[\eta_0(1+\eta_0)]^{1/2}\right\}\right]}{1 - \frac{R_+^0}{R_-^0} \exp\left\{\frac{2ik_0}{\eta_0}\chi\delta[\eta_0(1+\eta_0)]^{1/2}\right\}}, \tag{3a.11}$$

from which we obtain

$$|R(\chi\delta)|^2 = (R_+^0)^2 \frac{(1-\cos\gamma_0)^2 + \sin^2\gamma_0}{\left(1 - \frac{R_+^0}{R_-^0}\cos\gamma_0\right)^2 + \left(\frac{R_+^0}{R_-^0}\right)^2 \sin^2\gamma_0}, \tag{3a.12}$$

where we set, for short,

$$\gamma_0 \equiv \frac{2k_0}{\eta_0}\chi\delta[\eta_0(1+\eta_0)]^{1/2}. \tag{3a.13}$$

Formula (3a.12) can also be written as

$$|R(\chi\delta)|^2 = \frac{4(R_+^0)^2\tan^2(\gamma_0/2)}{[1+(R_+^0)^2]^2\tan^2(\gamma_0/2)+[1-(R_+^0)^2]^2} = \frac{\left(\dfrac{2R_+^0}{1-(R_+^0)^2}\right)^2\tan^2(\gamma_0/2)}{1+\left(\dfrac{1+(R_+^0)^2}{1-(R_+^0)^2}\right)^2\tan^2(\gamma_0/2)}, \tag{3a.12'}$$

where the relation $R_-^0 = 1/R_+^0$ has been used.

In the *deterministic* case, $\mu_0 = 1$, we have $\eta_0 = 1/\varepsilon$ and therefore

$$R_+^0 = -\left(1+\frac{2}{\varepsilon}\right)+\frac{2}{\varepsilon}(1+\varepsilon)^{1/2}, \qquad \gamma_0 = 2k_0\chi\delta(1+\varepsilon)^{1/2}.$$

As $R_-^0 = 1/R_+^0$, we have

$$\frac{2R_+^0}{1-(R_+^0)^2} = \frac{2}{R_-^0-R_+^0} = -\frac{1}{2[\eta_0(1+\eta_0)]^{1/2}} = -\frac{\varepsilon}{2(1+\varepsilon)^{1/2}},$$

$$\frac{1+(R_+^0)^2}{1-(R_+^0)^2} = \frac{R_-^0+R_+^0}{R_-^0-R_+^0} = \frac{1+2\eta_0}{2[\eta_0(1+\eta_0)]^{1/2}} = \frac{2+\varepsilon}{2(1+\varepsilon)^{1/2}},$$

and therefore

$$\left(\frac{2R_+^0}{1-(R_+^0)^2}\right)^2 = \frac{1}{4\eta_0(1+\eta_0)} = \frac{\varepsilon^2}{4(1+\varepsilon)},$$

$$\left(\frac{1+(R_+^0)^2}{1-(R_+^0)^2}\right)^2 = \frac{(1+2\eta_0)^2}{4\eta_0(1+\eta_0)} = \frac{(2+\varepsilon)^2}{4(1+\varepsilon)}.$$

Finally we obtain the formula

$$|R(\chi\delta)|^2 = \frac{\dfrac{\varepsilon^2}{4(1+\varepsilon)}\tan^2(\gamma_0/2)}{1+\dfrac{(2+\varepsilon)^2}{4(1+\varepsilon)}\tan^2(\gamma_0/2)} = \frac{\dfrac{\varepsilon^2}{(2+\varepsilon)^2}}{1+\dfrac{4(1+\varepsilon)}{(2+\varepsilon)^2}\cot^2[k_0\chi\delta(1+\varepsilon)^{1/2}]}, \tag{3a.14}$$

where $\gamma_0 \equiv 2k_0\chi\delta(1+\varepsilon)^{1/2}$. Here the fixed value δ can be replaced by *a continuous real variable* ranging over the whole interval $[0, \tau_{\max}]$. The parameter $\varepsilon > 0$ can also

take any value (not necessarily small) and also $\varepsilon < 0$ (plasmas), provided that $|\varepsilon| < 1$ (cf. [7, Sect. 25, p. 79, Problem 2] and also [11, Chap. 4, p. 97, formula (4.37)] for the Quantum Mechanical analogue).

Let us now return to the stochastic problem.

Remark 3a.3. Not every nonlinear (deterministic) ODE, even with constant coefficients, can be solved *explicitly* as in the case considered here. In general, we must proceed to the *numerical integration* of the (deterministic) equation under investigation, *for each realization.* Efficient ODE solvers do exist for this purpose.

Here is a description of the results. We chose up to $N = 100$ realizations and the parameter values $\varepsilon = 0.1$, $k_0 = 0.5$. Then we chose sections of unscaled length $\delta = \pi/2$, so that $s = 0.079577$, as the spectral density corresponding to the correlation function (3a.2′) can be computed explicitly by (3a.2):

$$s = \frac{k_0^2}{2} \frac{1 - \cos 2k_0 \delta}{4k_0^2 \delta} = \frac{1}{8\delta}. \tag{3a.15}$$

Therefore $\chi = 1256$ and, by choosing $p = 4700$ sections, we were able to cover scaled widths up to $\tau_{\max} = p\delta/\chi = 5.6$ (unscaled widths up to $l_{\max} = \chi\tau_{\max} \approx 7033$).

The error due to considering only $N = 100$ realizations is expected to be of order $O(N^{-1/2}) = O(10^{-1})$, by the central limit theorem (see Section 4).

Good agreement between the results of the simulation and those of the stochastic limit theory was already observed in [6, 9]. In [6], however, the realizations were constructed in such a way that the values ± 1 in each section were assigned according to an *exponential* distribution.

In the Figs. 1a–6a we plotted the results of the numerical simulations that we conducted with $\varepsilon = 0.1$, $k_0 = 0.5$ and the spectral density (3a.15) corresponding to the correlation function (3a.2′). The continuous curve indicates the result of the stochastic limit-theory (cf. [10]). In Fig. 1a we show the result obtained for a single

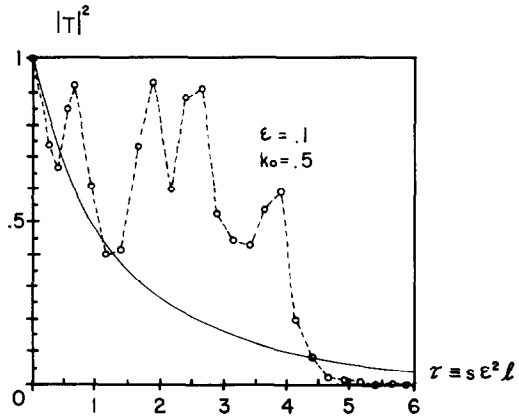

FIG. 1a. A single realization of $|T|^2$ vs $\tau \equiv s\varepsilon^2 l$, corresponding to a certain "seed."

realization for the transmitted power $|T|^2$ as a function of $\tau \equiv s\varepsilon^2 l$, corresponding to a certain "seed," chosen to start the generation of random numbers by means of a suitable routine on the computer. Such a routine is that one called GGUD in the IMSL package. It generates discrete uniformly distributed random numbers. We assume that different starting "seeds" as well as the "seed" automatically assigned by GGUD in the output (to be used in a subsequent call) yield *uncorrelated* sequences of (pseudo-) random numbers. In Figs. 2a, 3a, and 4a we show the results obtained by averaging over 10, 40 and 100 realizations, respectively. In Figs. 5a and 6a, finally, we show two other realizations of $|T|^2$, obtained by assigning different "seeds."

Single realizations can be thought of as corresponding to solutions of *deterministic* problems, though likely with a very irregular refractive index. Note that in such a case $|T|^2$ may become quite "large," close to 1, for $\tau > 0$. In fact, in the deterministic lossless case, *resonances* may occur for certain values of the ratio l/λ, λ being the wavelength of the wave propagating through the slab, $\lambda = 2\pi/k$, when $1 + \varepsilon\mu \equiv \text{const}$, $k = k_0(1 + \varepsilon\mu)^{1/2}$, and then (almost) all power could go through the slab.

The situation is quite different in the *stochastic* problem. There is a clear *numerical evidence* that, if we consider a sufficiently large number of realizations, the corresponding average of $|T|^2$ decays fast to zero, as $\tau \equiv s\varepsilon^2 l \to \infty$. This agrees with the stochastic *limit-theory*, where it is shown that $\langle |T|^2 \rangle$ decays *exponentially* as $\tau \to \infty$ (localization); cf. [5, 6, 8–10]. The physical explanation lies in the fact that, as the medium is assumed to be lossless, the power cannot be absorbed nor anyway dissipated by the medium itself. Therefore a half-space of such a medium must reflect back *all* the incident power.

3b. *Numerical Simulation for a Linear BV-Problem for a Second Order* SODE

The technique adopted here consists of constructing again several realizations of the process μ, according to its statistical properties, by generating on the computer

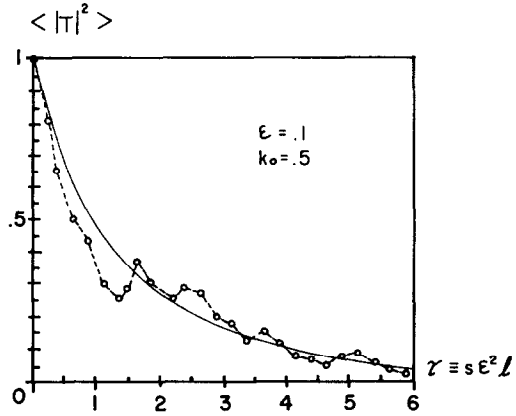

FIG. 2a. $\langle |T|^2 \rangle$ over 10 realizations vs $\tau \equiv s\varepsilon^2 l$.

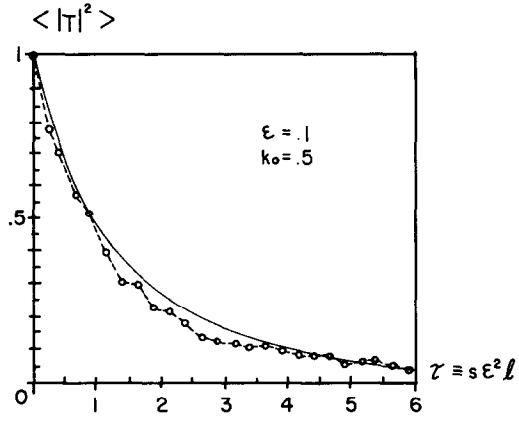

FIG. 3a. $\langle |T|^2 \rangle$ over 40 realizations vs $\tau \equiv s\varepsilon^2 l$.

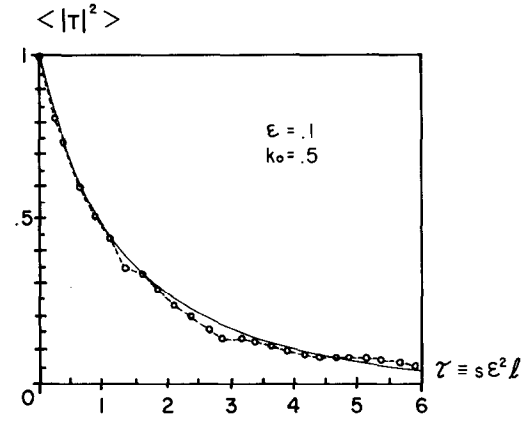

FIG. 4a. $\langle |T|^2 \rangle$ over 100 realizations vs $\tau \equiv s\varepsilon^2 l$.

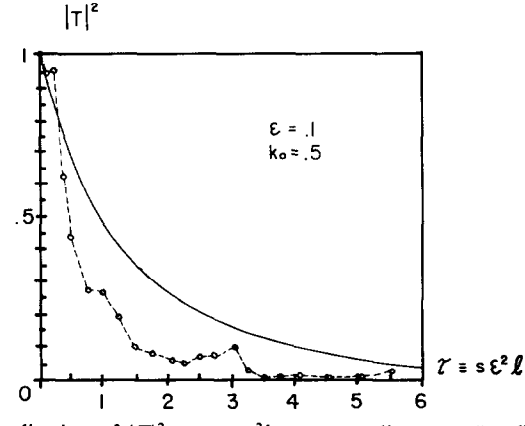

FIG. 5a. A single realization of $|T|^2$ vs $\tau \equiv s\varepsilon^2 l$, corresponding to a "seed" different from that of Fig. 1a.

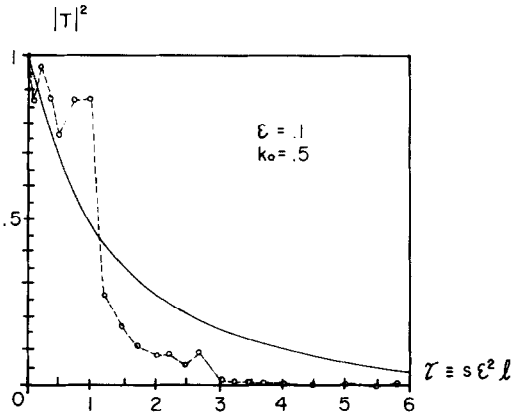

FIG. 6a. A single realization of $|T|^2$ vs $\tau \equiv s\varepsilon^2 l$, corresponding to a "seed" different from those in Figs. 1a and 5a.

suitable sequences of random numbers, and solving Eq. (2.1) with the boundary conditions (2.3'), by using *propagator matrices*. That is, we express the general solution of (2.1), in each section where μ is constant, by means of a fundamental matrix solution and multiply all these matrices. The boundary conditions are then imposed.

In practice, we again divide $[0, l_{\max}]$ into p sections of equal length $\Delta = l_{\max}/p$, where $\mu = \pm 1$, with the sign $\pm$ chosen at random, and thus

$$h_j = k_0[1 + \varepsilon\mu_j]^{1/2} \tag{3b.1}$$

is the refractive index in the jth section (cf. Section 3a).

For each q, $1 \leqslant q \leqslant p$, we solve a BV-problem in the interval $[0, l_q]$, where $l_q \leqslant l_p \equiv l_{\max}$. Writing Eq. (2.1) as a system for the vector

$$\mathbf{z}_l(x) \equiv \begin{bmatrix} u(x) \\ u_x(x) \end{bmatrix}, \tag{3b.2}$$

if $0 \equiv x_0 < x_1 < x_2 < \cdots < x_{q-1} < x_q \equiv l_q$ denotes an increasing sequence of points, the solution at $x = x_1$ can be expressed as

$$\mathbf{z}_l(x_1) = \mathbf{M}(x_1, x_0)\, \mathbf{z}_l(x_0), \tag{3b.3}$$

where

$$\mathbf{M}(x_1, x_0) = \begin{bmatrix} \cos[h_1(x_1 - x_0)] & (1/h_1)\sin[h_1(x_1 - x_0)] \\ -h_1 \sin[h_1(x_1 - x_0)] & \cos[h_1(x_1 - x_0)] \end{bmatrix} \tag{3b.4}$$

is the *fundamental matrix solution* of the equation for $\mathbf{z}_l(x)$. The solution at $x = x_2$ can be written as

$$\mathbf{z}_l(x_2) = \mathbf{M}(x_2, x_1)\, \mathbf{z}_l(x_1) = \mathbf{M}(x_2, x_1)\, \mathbf{M}(x_1, x_0)\, \mathbf{z}_l(x_0), \tag{3b.3'}$$

where

$$\mathbf{M}(x_2, x_1) = \begin{bmatrix} \cos[h_2(x_2 - x_1)] & (1/h_2)\sin[h_2(x_2 - x_1)] \\ -h_2 \sin[h_2(x_2 - x_1)] & \cos[h_2(x_2 - x_1)] \end{bmatrix} \tag{3b.4'}$$

and, in general

$$\begin{aligned} \mathbf{z}_l(x_q) &= \mathbf{M}(x_q, x_{q-1})\, \mathbf{z}_l(x_{q-1}) = \cdots \\ &= \mathbf{M}(x_q, x_{q-1})\, \mathbf{M}(x_{q-1}, x_{q-2}) \cdots \mathbf{M}(x_2, x_1)\, \mathbf{M}(x_1, x_0)\, \mathbf{z}_l(x_0). \end{aligned} \tag{3b.5}$$

Therefore we have

$$\mathbf{z}_l(x_q) = \left(\prod_{m=1}^{q} \mathbf{M}(x_{q-m+1}, x_{q-m}) \right) \mathbf{z}_l(x_0) = \mathbf{M}_q \mathbf{z}_l(x_0). \tag{3b.6}$$

The boundary conditions are imposed at this point. By specializing the procedure above to our problem, by assuming $x_m - x_{m-1} = \Delta$, $m = 1, 2, ..., q$, we have

$$\mathbf{M}(x_m, x_{m-1}) \equiv \mathbf{M}_m(\Delta, 0), \qquad m = 1, 2, ..., q. \tag{3b.7}$$

By using the boundary conditions (2.3'), we get

$$\mathbf{z}_0 \equiv \begin{bmatrix} u(0) \\ u_x(0) \end{bmatrix} = \begin{bmatrix} 1 \\ -ik_0 \end{bmatrix} u(0), \tag{3b.8'}$$

$$\mathbf{z}_l \equiv \begin{bmatrix} u(l_q) \\ u_x(l_q) \end{bmatrix} = \begin{bmatrix} u(l_q) \\ ik_0 u(l_q) - 2ik_0 \end{bmatrix} = \begin{bmatrix} 1 \\ ik_0 \end{bmatrix} u(l_q) - 2ik_0 \begin{bmatrix} 0 \\ 1 \end{bmatrix}, \tag{3b.8''}$$

i.e., by using (3b.6),

$$\begin{aligned} u(l_q) &= M_{11} u(0) - M_{12} ik_0 u(0) \\ ik_0 u(l_q) - 2ik_0 &= M_{21} u(0) - M_{22} ik_0 u(0), \end{aligned} \tag{3b.9}$$

where M_{ij} are the entries of $\mathbf{M}$. By eliminating $u(0)$, we obtain

$$\begin{aligned} u(0) &= \frac{1}{\alpha} u(l_q), \\ u(l_q) &= \frac{2ik_0 \alpha}{ik_0 \alpha - \beta}, \end{aligned} \tag{3b.10}$$

where we set, for short,

$$\begin{aligned} \alpha &\equiv M_{11} - ik_0 M_{12}, \\ \beta &\equiv M_{21} - ik_0 M_{22}. \end{aligned} \tag{3b.11}$$

As we are mainly interested in the reflection coefficient, we can compute (cf. (2.5))

$$R_q \equiv u(l_q) - 1 = \frac{ik_0\alpha + \beta}{ik_0\alpha - \beta} = \frac{1 + \dfrac{i\beta}{k_0\alpha}}{1 - \dfrac{i\beta}{k_0\alpha}}, \tag{3b.12}$$

and then $|R_q|^2 \equiv R_q R_q^*$ and $|T_q|^2 \equiv 1 - |R_q|^2$.

It is also of some interest for its physical meaning and to observe "what happens" inside the slab, to compute the *total power* or *intensity*

$$P(x) \equiv |u(x)|^2 + \frac{1}{k_0^2}|u_x(x)|^2, \tag{3b.13}$$

for a fixed l, $0 < l \leqslant l_{\max}$ and $0 \leqslant x \leqslant l$.

All this procedure must be repeated for several realizations and then the averages of $|R_q|^2$, $|T_q|^2$, P over such realizations will be computed. In Figs. 1b–6b we show the results. The parameters $k_0 = 0.5$, $\varepsilon = 0.3$ and $p = 500$ (the number of sections) were used throughout. The higher value for ε and the smaller value for p, in comparison with the computations reported in Section 3a, were chosen to contain the "cost," which here is higher than there. The results are qualitatively the same, even though the convergence to the "true" (exact) solution to the stochastic limit-problem (shown by the continuous curve drawn for comparison on each graph) is slower.

In Fig. 1b we show the result for $|T|^2$ corresponding to a single realization

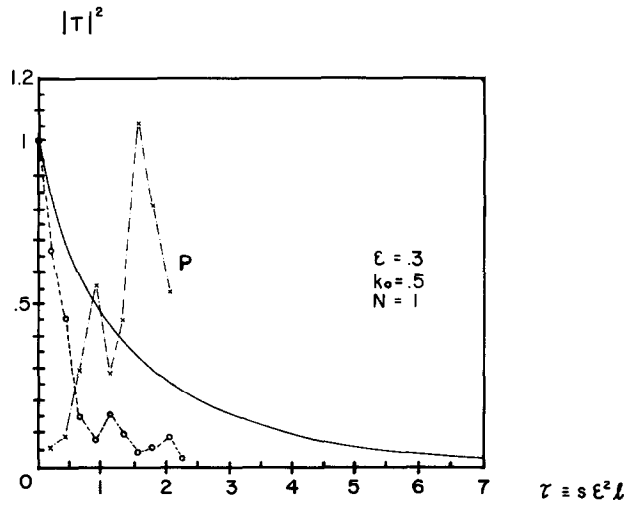

FIG. 1b. A single realization of $|T|^2$ and of $P \equiv |u|^2 + k_0^{-2}|u_x|^2$ vs $\tau \equiv s\varepsilon^2 l$, corresponding to a certain "seed."

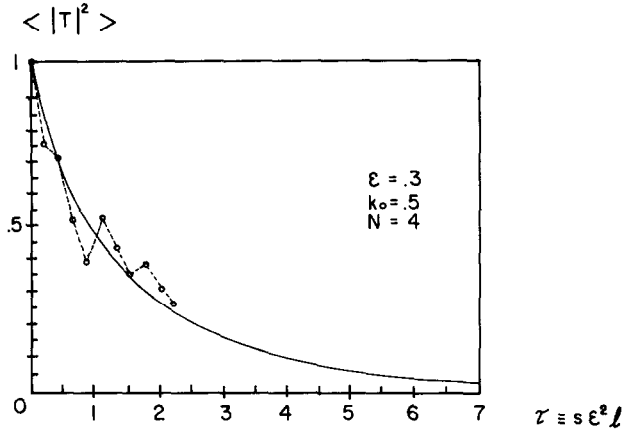

FIG. 2b. $\langle |T|^2 \rangle$ over 4 realizations vs $\tau \equiv s\varepsilon^2 l$.

($N = 1$) obtained by assigning some "seed" in the routine GGUD which generates the sequence of random ± 1's. The "total power" defined in (3b.13) is also shown. In Figs. 2b, 3b, and 4b′, we show the average $\langle |T|^2 \rangle$ of the transmitted power over $N = 4$, 10 and 40 realizations, respectively. In this last figure the "total power" is also plotted. In Fig. 4b″, $\langle |T|^2 \rangle$ is computed again over $N = 40$ realizations, but starting from a different "seed." In Fig. 5b we plot the quantity $\langle |T|^2 \rangle$ computed over $N = 100$ realizations, while in Figs. 6b′ and 6b″ we show respectively the average over $N = 80$ realizations (where the first 40 correspond to Fig. 4b″), and over $N = 120$ realizations (with the first 80 corresponding to Fig. 6b′).

From all of these graphs we can have a clear though only qualitative idea about the convergence and the numerical error, because we *know* the true limiting-

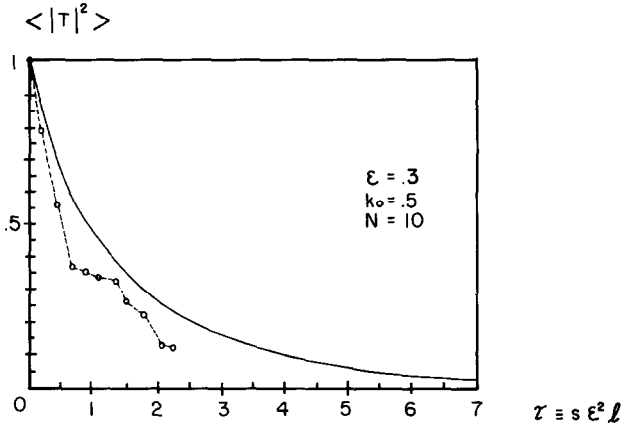

FIG. 3b. $\langle |T|^2 \rangle$ over 10 realizations vs $\tau \equiv s\varepsilon^2 l$.

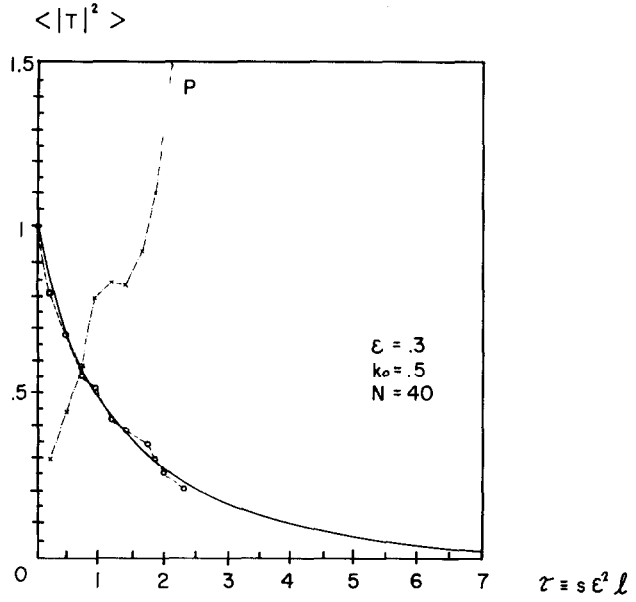

FIG. 4b'. $\langle |T|^2 \rangle$ and $\langle P \rangle \equiv \langle |u|^2 + k_0^{-2}|u_x|^2 \rangle$ over 40 realizations vs $\tau \equiv s\varepsilon^2 l$.

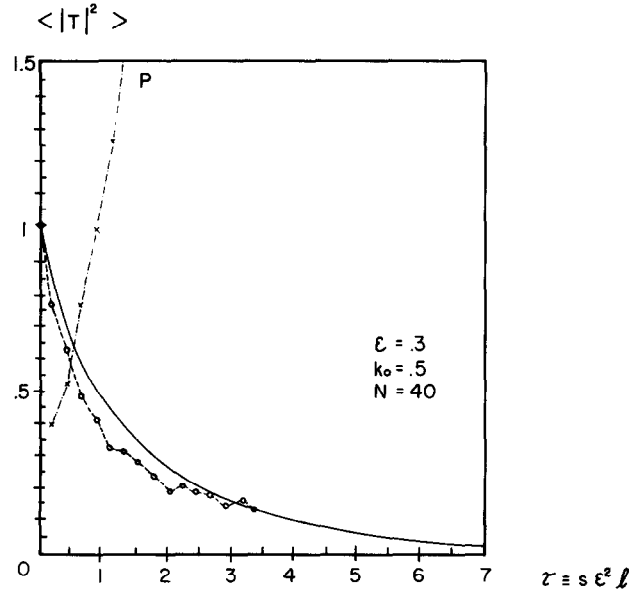

FIG. 4b". $\langle |T|^2 \rangle$ and $\langle P \rangle \equiv \langle |u|^2 + k_0^{-2}|u_x|^2 \rangle$ over 40 realizations, vs $\tau \equiv s\varepsilon^2 l$ but starting from a "seed" different from that in Fig. 4b'.

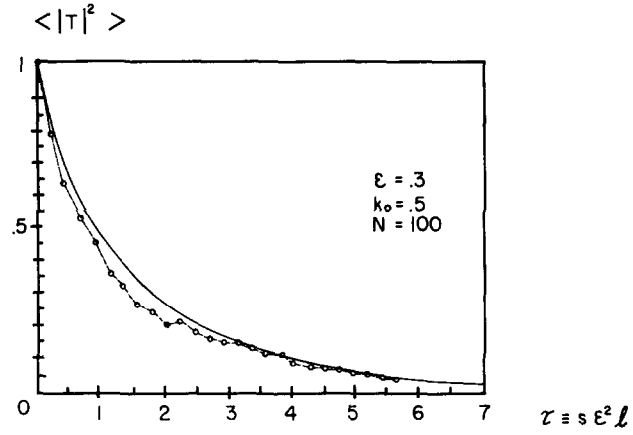

FIG. 5b. $\langle |T|^2 \rangle$ over 100 realizations vs $\tau \equiv s\varepsilon^2 l$.

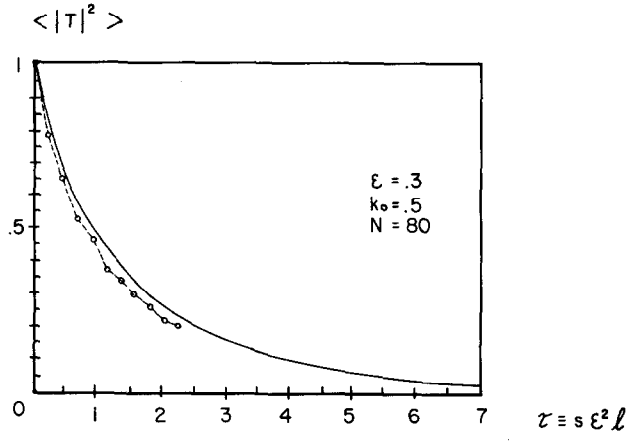

FIG. 6b'. $\langle |T|^2 \rangle$ over 80 realizations (where the first 40 correspond to Fig. 4b"), vs $\tau \equiv s\varepsilon^2 l$.

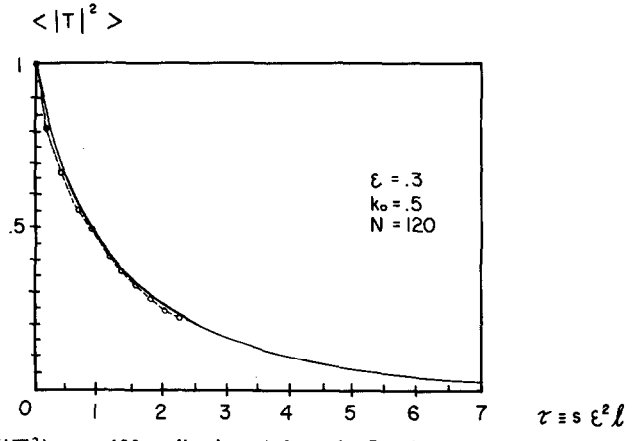

FIG. 6b". $\langle |T|^2 \rangle$ over 120 realizations (where the first 80 correspond to Fig. 6b'), vs $\tau \equiv s\varepsilon^2 l$.

solution but we do not make any comparison with the *exact* solution to the problem with ε, l *fixed* (rather than $\varepsilon \to 0$, $l \to \infty$). Questions about convergence and errors will be addressed in the next section.

4. About the Errors

Besides the usual *truncation* (or "discretization") and *round-off* errors that we meet solving, e.g., differential equations by implementing numerical algorithms, here we have to take into account some additional sources of error, due to the statistical nature of the method we used.

First of all we have to consider that we generate on the computer sequences of random numbers, according to some statistics. Suppose that we want to generate Gaussian (normal) random variables. In practice, however, the physical devices and the existing routines are unable to generate a perfectly Gaussian variable, say $\xi(\omega)$: They will produce, rather, some random variable $\eta(\omega)$ such that

$$\eta(\omega) = \xi(\omega) + \delta(\omega), \tag{4.1}$$

where the error term $\delta(\omega)$ can be assumed uncorrelated with $\xi(\omega)$ (cf. [12]). Here $\omega \in \Omega$ represents the "chance," ranging over some abstract space Ω, which is part of the triplet $(\Omega, \mathcal{A}, P)$, the underlying probability space. Moreover it is reasonable to assume that $\langle \delta(\omega) \rangle = 0$, while $\langle \delta^2(\omega) \rangle = O(1/N)$, N being the number of the realizations, besides $\langle \xi(\omega)\, \delta(\omega) \rangle = 0$.

Furthermore, we approximate the expected value of a certain quantity, i.e, an integral over some space (Ω), with respect to some probability measure (P), by an average over a finite number N of realizations. This is the *finite sampling error*, due to the finite size of any sample that must necessarily be used. Suppose that $\xi_1(\omega)$, $\xi_2(\omega)$, ..., $\xi_N(\omega)$ are N independent identically distributed random variables, with two finite moments μ, σ. Then the strong (and weak) law of large numbers holds, as well as the classical central limit theorem. Therefore, if $s_N(\omega) = \sum_{i=1}^{N} \xi_i(\omega)$, then

$$P\left(\lim_{N \to \infty} \frac{s_N(\omega)}{N} = \mu \right) = 1, \tag{4.2}$$

and

$$\lim_{N \to \infty} P\left(\frac{s_N(\omega) - N\mu}{\sigma \sqrt{N}} \leqslant x \right) = \frac{1}{\sqrt{2\pi\sigma}} \int_{-\infty}^{x} e^{-y^2/2}\, dy. \tag{4.3}$$

Therefore: (i) the arithmetic mean $s_N(\omega)/N$ of the $\xi_i(\omega)$'s converges to the expected value μ of each $\xi_i(\omega)$, with probability 1, and (ii) the random variable $(s_N(\omega) - N\mu)/(\sigma \sqrt{N})$ converges in distribution to a Gaussian (normal) random variable. Equation (4.2) justifies taking the arithmetic mean, for every x, instead of

the expected value, and (4.3) justifies, in some sense, assuming that the error between the arithmetic mean and the expected value is of order $O(1/\sqrt{N})$.

Besides computing the *average*

$$G_1(x_j) \equiv \frac{1}{N} \sum_{i=1}^{N} g_i(x_j), \qquad j = 1, 2, ..., p, \tag{4.4}$$

of the realizations g_i at any fixed value x_j, that is a candidate for approximating the *expected value* of the process $g(x, \omega)$ at $x = x_j$, we compute the quantity

$$G_2(x_j) \equiv \frac{1}{N} \sum_{i=1}^{N} g_i^2(x_j), \qquad j = 1, 2, ..., p. \tag{4.5}$$

In our problem $g_i(x_j) = |R_i(x_j)|^2$.

It is reasonable to think that G_2 represents the *estimated* second moment. Then, if we compute

$$\sigma_g(x_j) \equiv \left[\frac{1}{N-1} (G_2(x_j) - G_1^2(x_j)) \right]^{1/2}, \tag{4.6}$$

σ_g^2 is the *estimated* variance, and the ratio σ_g/G_1, called the *coefficient of variation*, is generally accepted as a good measure of the (relative) sampling error; it can be given in percentages (cf. [3]). The appearance of $N-1$ instead of N is required in order to have an *unbiased* estimator; when $N \gg 1$ the difference is, of course, irrelevant.

Therefore the error to be computed is

$$E \equiv \max_{1 \le j \le p} \left\{ \frac{\sigma_g(x_j)}{G_1(x_j)} \right\}. \tag{4.7}$$

In our problem we obtained $E \approx 11.2\%$ with $N = 100$ realizations, in case (b). Observe, however, that $N = 100$ realizations and the consequent low computational cost is very little for Monte Carlo simulations standards.

Note. In the figures the solid line refers to the stochastic limit-theory [10]. However, this represents the "true" solution only when ε is sufficiently small and l is sufficiently large.

We should also consider that computing averages over a large number of realizations introduces additional *round-off* errors, with respect to the corresponding deterministic case (cf. [12]). This error may become important when the sample size is very large.

Several experiments seem to show that finite sampling and, perhaps, the last quoted round-off error dominate the others (cf. [12]).

5. Summary

In closing, let us summarize the major points of the paper. A Monte Carlo simulation technique has been adopted for numerically solving certain problems of wave propagation in random media, governed by stochastic ordinary differential equations. This approach is very simple and quite general: It is (trivially) suited to parallel computing and preserves the correct probabilistic structure of the problem. It can be used for solving more general stochastic ordinary differential equations, and is useful especially when no other methods are available. Moreover, in many cases it can be also computationally very cheap.

Besides illustrating with several pictures the results relevant to the particular physical problem we considered, we have discussed the various sources of errors that beset our method and estimated the most important errors.

All the computations were performed on CDC/Cyber 170, at the Courant Institute of Mathematical Sciences, New York University.

References

1. G. I. Babkin and V. I. Klyatskin, *Sov. Phys.-JETP* **52** (3), 416 (1980) [Transl. from *Zh. Exsp. Teor. Fiz.* **79**, 817 (1980)].
2. G. I. Babkin and V. I. Klyatskin, *Wave Motion* **4**, 195 (1982).
3. J. M. Hammersley and D. C. Handscomb, *Monte Carlo Methods* (Methuen, London and Wiley, New York, 1964).
4. R. Z. Kahsminskii, *Theory Probab. Appl.* **11**, 390 (1966).
5. W. Kohler and G. C. Papanicolaou, *J. Math. Phys.* **14**, 1733 (1973).
6. W. Kohler and G. C. Papanicolaou, *J. Math. Phys.* **15**, 2186 (1974).
7. L. D. Landau and E. M. Lifshitz, *Quantum Mechanics (Nonrelativistic Theory)* (Pergamon, Oxford, 1977, 3rd ed.).
8. D. Marcuse, *IEEE Trans. Microwave Theory Technol.* **20**, 541 (1972).
9. J. A. Morrison, *IEEE Trans. Microwave Theory Technol.* **22**, 126 (1974).
10. G. C. Papanicolaou, *SIAM J. Appl. Math.* **21**, 13 (1971).
11. D. Park, *Introduction to the Quantum Theory* (McGraw-Hill, New York, 1974, 2nd ed.).
12. J. R. Klauder and W. P. Petersen, *SIAM J. Numer. Anal.* **22**, 1153 (1985).
13. R. Spigler, *J. Comput. Phys.* **73**, Prod. Ed.; PN 2551 (1987).